Journal of Neuroscience Research 77:762–769 (2004)

High-Resolution Magic Angle Spinning and ^{1}H Magnetic Resonance Spectroscopy Reveal Significantly Altered Neuronal Metabolite Profiles in CLN1 but Not in CLN3

Beathe Sitter,[1,2] Taina Autti,[3] Jaana Tyynelä,[4,5] Ursula Sonnewald,[2] Tone F. Bathen,[1] Johanna Puranen,[3] Pirkko Santavuori,[6] Matti J. Haltia,[5] Anders Paetau,[5] Tuomo Polvikoski,[5] Ingrid S. Gribbestad,[1] and Anna-Maija Häkkinen[3,7]★

[1]SINTEF Unimed, Trondheim, Norway
[2]Department of Neuroscience, NTNU, Trondheim, Norway
[3]Department of Radiology, Helsinki University Central Hospital, Helsinki, Finland
[4]Institute of Biomedicine/Biochemistry and Neuroscience Research Program, University of Helsinki, Helsinki, Finland
[5]Department of Pathology, Haartman Institute and Helsinki University Central Hospital, Helsinki, Finland
[6]Department of Child Neurology, Helsinki University Central Hospital, Helsinki, Finland
[7]Department of Oncology, Helsinki University Central Hospital, Helsinki, Finland

The neuronal ceroid lipofuscinoses (NCLs) are among the most severe inherited progressive neurodegenerative disorders of children. The purpose of this study was to compare the in vivo 1.5-T ^{1}H magnetic resonance (MR) and ex vivo 14.3-T high-resolution (HR) magic angle spinning (MAS) ^{1}H MR brain spectra of patients with infantile (CLN1) and juvenile (CLN3) types of NCL, to obtain detailed information about the alterations in the neuronal metabolite profiles in these diseases and to test the suitability of the ex vivo HR MAS ^{1}H MRS technique in analysis of autopsy brain tissue. Ex vivo spectra from CLN1 autopsy brain tissue (n = 9) significantly differed from those of the control (n = 9) and CLN3 (n = 5) groups, although no differences were found between the CLN3 and the control groups. Principal component analysis of ex vivo data showed that decreased levels of *N*-acetylaspartate (NAA), γ-aminobutyric acid (GABA), glutamine, and glutamate as well as increased levels of inositols characterized the CLN1 spectra. Also, the intensity ratio of lipid methylene/methyl protons was decreased in spectra of CLN1 brain tissue compared with CLN3 and control brain tissue. In concordance with the ex vivo data, the in vivo spectra of late-stage patients with CLN1 (n = 3) revealed a dramatic decrease of NAA and a proportional increase of myo-inositol and lipids compared with control subjects. Again, the spectra of patients with CLN3 (n = 13) did not differ from those of controls (n = 15). In conclusion, the ex vivo and in vivo spectroscopic findings were in good agreement within all analyzed groups and revealed significant alterations in metabolite profiles in CLN1 brain tissue but not in CLN3 compared with controls. Furthermore, HR MAS ^{1}H MR spectra facilitated refined detection of neuronal metabolites, including GABA, and composition of lipids in the autopsy brain tissue of NCL patients.

Key words: neuronal ceroid lipofuscinosis; magic angle spinning; principal component analysis

Neuronal ceroid lipofuscinoses (NCLs) are recessively inherited storage diseases, and they are the most common reason for progressive childhood encephalopathies leading to death (Mole, 1999; Hofmann and Peltonen, 2001; Haltia, 2003). All forms of NCLs are characterized by lysosomal storage of autofluorescent lipopigments in several types of tissues, particularly in neurons of the central nervous system (Haltia, 2003). Another typical feature of NCLs is the progressive neurodegeneration. At present, altogether, eight different forms of NCL have been postulated (Mole, 1999; Hofmann and Peltonen, 2001). Six genes and the respective proteins underlying the NCLs have been identified (International Batten Disease Consortium, 1995; Vesa et al., 1995; Sleat et al., 1997; Savukoski et al., 1998; Ranta et al., 1999; Gao et al., 2002; Wheeler et al., 2002). Among these are the palmitoyl protein thioesterase 1 (PPT1) and CLN3 protein, defects of which cause infantile NCL (CLN1 or INCL) and juvenile NCL (CLN3 or JNCL), respectively (International

Contract grant sponsor: Academy of Finland; Contract grant number: JT 207016; Contract grant sponsor: University of Helsinki Research Funds; Contract grant number: JT 2103029.

★Correspondence to: Anna-Maija Häkkinen, Department of Oncology, POB 180, 00029 Helsinki University Central Hospital, University of Helsinki, Helsinki, Finland. E-mail: anna-maija.hakkinen@hus.fi

Received 13 June 2003; Revised 9 February 2004; Accepted 12 February 2004

Published online 13 July 2004 in Wiley InterScience (www.interscience.wiley.com). DOI: 10.1002/jnr.20123

Batten Disease Consortium, 1995; Vesa et al., 1995). Infantile CLN1 is a rapidly progressing form, with extreme brain atrophy and life expectancy of 8–14 years, whereas juvenile CLN3 is associated with moderate brain atrophy and life expectancy of 16–35 years. The frequencies of CLN1 and CLN3 vary among different populations: CLN1 is enriched in Finland, with an incidence of 1:18,000, whereas the incidence of CLN3 is 1:21,000 in Finland and 1:25,000 in the northern European countries (Santavuori, 1988; Hofmann and Peltonen, 2001).

In vivo magnetic resonance imaging (MRI) and spectroscopy (MRS) have been used in differential diagnosis between NCLs and other neurodegenerative diseases (Confort-Gouny et al., 1993; Brockmann et al., 1996; Autti et al., 1997; Seitz et al., 1998; Lauronen et al., 1999). High-resolution MR spectra can provide detailed and complex information on the biochemical composition of the tissue under investigation. The magic angle spinning (MAS) technique facilitates a high-resolution MRS (HR MRS) of tissue samples ex vivo, eliminating the need for metabolite extraction (Sitter et al., 2002). HR MAS ^{1}H MR spectra have resolution comparable to spectra of solutions and provide information about a larger number of metabolites than in vivo MR spectra. In biomedical research, ex vivo HR MAS ^{1}H MRS has been successfully applied in studies on various human tissues and diseases, including breast cancer (Cheng et al., 1998; Sitter et al., 2002), prostate carcinomas (Cheng et al., 2001; Taylor et al., 2003), and brain tumors (Barton et al., 1999; Cheng et al., 2000; Tzika et al., 2002). Ex vivo HR MAS ^{1}H MRS has also been used for characterization of neuronal loss in a macaque model of AIDS (Gonzales et al., 2000), Pick's disease (Cheng et al., 1997), and Alzheimer's disease (Cheng et al., 2002).

The vast amount of metabolites detected in HR MAS ^{1}H MR spectra makes visual inspection and analysis difficult. In addition to handling large data sets, multivariate analysis, such as principal component analysis (PCA), has the potential to detect small variations between spectra. The aims of the present study were to compare the in vivo 1.5-T ^{1}H MR and ex vivo 14.3-T HR MAS ^{1}H MR brain spectra of patients with CLN1 and CLN3, to obtain detailed information about the alterations in the neuronal metabolite profiles in these diseases and to test the suitability of the ex vivo HR MAS ^{1}H MRS technique in analysis of autopsy brain tissue.

MATERIALS AND METHODS

Subjects

Informed consent was obtained from the parents of the patients and from the controls or their families. The local ethical committee approved the study protocol. Three late-stage patients with CLN1 (ages 4, 6, and 7 years), 13 patients with CLN3 (median age 14 years, range from 7 to 30 years, 5 patients $<$12 years and 8 $>$12 years old), and 15 healthy volunteers (median age 22 years, range from 7 to 35 years) were examined by in vivo ^{1}H MRS. All patients with CLN1 (two girls and one boy) were markedly affected and had been unable to move since the age of 2.5 years. They all had epilepsy and myoclonic jerks. Patients with CLN3 (eight boys and five girls) under 12 years had only visual failure and slight cognitive decline, whereas older patients (except for one) had epilepsy, motor and speech problems, and marked cognitive decline. The controls (one girl, nine men, and five women) were healthy and had no neurological deficits.

Autopsy samples for ex vivo MR spectroscopy were excised from the frontal cortices of patients with CLN1 and CLN3 and controls without neurological deficits. Samples were frozen and stored at −80°C until analysis. The group of patients with CLN1 (n = 9) consisted of two boys and seven girls with a median age of 11 years at the time of death (range 10.6–15 years). All had had myoclonic epilepsy and had been severely affected and bedridden since the age of 2.5 years. Dystonia had also been common. The patients with CLN3 (n = 5) were two men and three women who died at a median age of 27 years (range from 20 to 36 years). During the second decade of their life, three of them had shown a more rapid clinical course than the others (Järvelä et al., 1997). The control group (n = 9) consisted of six women and three men who had no neurological deficits, and their median age was 92 years at death (range from 36 to 106 years). Mini-Mental State Examination or Short Portable Mental Status Questionnaire were used to assess the cognitive status of the old controls ($>$85 years of age), and they were not cognitively impaired, nor did they show any gross pathology in the forebrain as confirmed by neuropathological examination (Polvikoski et al., 2001).

In Vivo ^{1}H MRS

Localized single-voxel ^{1}H MR spectra were recorded on a 1.5-T (63-MHz) Magnetom Vision MR imager (Siemens, Erlangen, Germany) by using a standard, circularly polarized head coil. The thalamic nuclei were examined by using in vivo ^{1}H MRS. The size of the selected volume of interest ranged from 4 to 8 cm^{3}. A stimulated echo acquisition mode (STEAM) sequence with selective water suppression was used for MRS. The echo time (TE) was 270 msec and 20 msec, repetition time (TR) 3,000 msec, and mixing time (TM) 30 msec. Unsuppressed tissue water signal was also collected with TR of 5,000 msec in the corresponding voxel. The metabolite spectra were acquired by using 256 (TE = 270 msec) and 128 (TE = 20 msec) acquisitions, and eight acquisitions for tissue water, over a spectral region of 1,000 Hz collected into 1,024 data points. The chemical shifts were referenced to water at 4.75 ppm. The cerebral metabolite signal intensities were determined by using frequency domain fitting with Siemens software and, for CLN1, also with SPW software (Järvi et al., 1997). For comparison of the spectra of the different individuals, the signal intensities were corrected for coil loading and VOI size.

Ex Vivo HR MAS ^{1}H MRS

HR MAS ^{1}H MR spectra of autopsy brain samples were recorded using a Bruker Avance DRX600 (14.3-T) spectrometer equipped with a ^{1}H/^{13}C MAS probe with gradient directed along the magic angle axis (Bruker Analytik GmbH). Samples were spun at 3.5 kHz. All spectra were recorded at room temperature.

Two different one-dimensional spectra were recorded for each sample. A spin echo experiment with water suppression

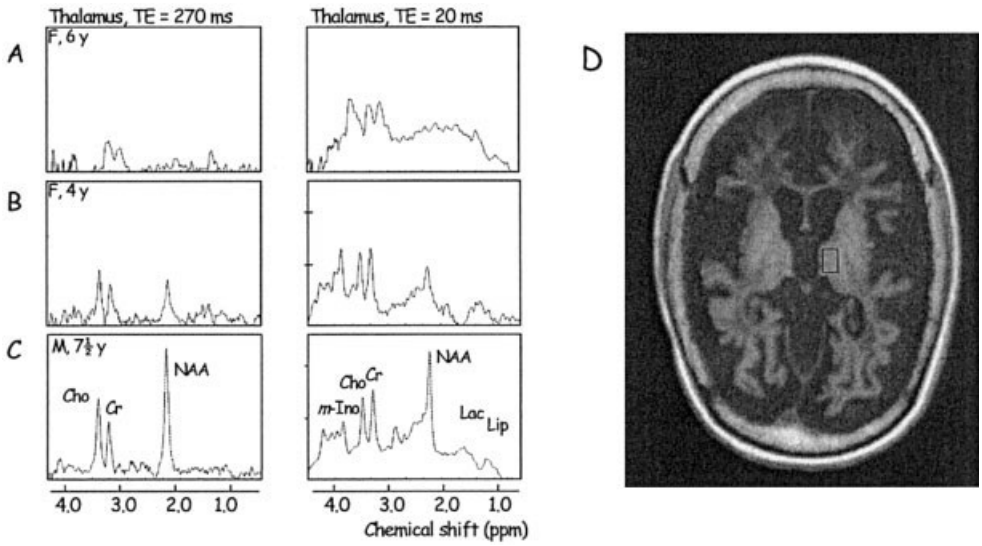

Fig. 1. In vivo ^{1}H spectra at 1.5 T (63 MHz) of 6-year-old (**A**) and 4-year-old (**B**) patients with CLN1 show decreases of NAA and proportional increases of m-Ino and Cho compared with the spectra of a 7.5-year-old healthy control (**C**). m-Ino, myo-inositol; Cho, cholines; Cr, creatines; NAA, *N*-acetyl-aspartate; Lac, lactate; Lip, lipids. The MRI (T1-weighted image) of the 6-year-old patient (**D**) shows extremely severe brain atrophy. The thalami are best preserved, but the cerebral cortex is very thin. MRS localization is marked by a rectangle.

included (cpmgpr; Bruker) was performed with a delay of 1 msec, repeated 136 times, giving spectra with a total echo time of 285 msec. The second type of spectra was acquired by using a single pulse sequence with water suppression (zgpr; Bruker). The water resonance was irradiated for 2 sec before a 60° pulse angle was applied. For both experiments, 128 transients over a spectral region of 10 kHz were collected into 32,000 points, giving an acquisition time of 1.64 sec. All experiments were performed at room temperature. Chemical shifts were referenced to creatine (3.03 ppm).

Before multivariate analysis, all spectra were Fourier transformed, and baseline offset was adjusted. From the spin echo spectra, the spectral region from 0.6 to 4.6 ppm was selected for multivariate analysis. From the single pulse water-suppressed spectra, the spectral region between 0.8 and 3.5 ppm was selected. The region describing the lactate peak at 1.32 ppm (40 points) was removed from all spectra because of the much higher signal intensity compared with the rest of the spectrum. The final matrix of spin echo spectra consisted of 25 samples × 3,810 variables, whereas the final matrix of single pulse spectra consisted of 25 samples × 2,610 variables. Mean normalization was performed on the selected spectral regions. PCA was carried out in an unsupervised manner, with full cross-validation and mean centering with the program The Unscrambler from Camo.

The program PeakFit from Jandel Scientific was used to calculate areas of the methyl (CH_3, 0.9 ppm) and methylene (CH_2, 1.3 ppm) signals from fatty acids in the single pulse (water-suppressed) spectra. The spectral region of 1.8–0.5 ppm was used, and all peaks in this region were fitted to a combined Lorenzian-Gaussian line shape ($r^2 > 0.99$). ANOVA was used to test the resulting methylene/methyl ratios of lipids for statistical significance.

RESULTS

In Vivo ^{1}H MRS

In the patients with CLN1 (ages 4, 6, and 7 years), the metabolites measured from thalami (Fig. 1) showed markedly altered intensities: *N*-acetylaspartate (NAA) was only 40%, 15%, and 30%; creatine + phosphocreatine (Cr) 80%, 50%, and 70%; and choline-containing compounds (Cho) 110%, 120%, and 90%, respectively, of the control (TE = 270 msec). The proportional intensities of inositols, composed mainly of myo-inositol (m-Ino), and of lipids (TE = 20 msec) were markedly higher in CLN1 than in the control. In addition, the lactate signal was detectable in CLN1 (TE = 270 msec). In contrast, the spectra of the CLN3 patients did not differ from those of the controls. The mean values ± SD for NAA in CLN3 patients and controls were 29 ± 6 and 29 ± 5 institutional units (i.u.), for Cr 11 ± 3 and 10 ± 2 i.u., and for Cho 12 ± 4 and 9 ± 2 i.u., respectively (TE = 270 msec).

Ex Vivo HR MAS ^{1}H MRS

Typical spin echo HR MAS ^{1}H MR spectra (spectral region 4.6–0.6 ppm) of autopsy tissue of the frontal cortex from patients with CLN1 and CLN3 and control subjects are presented in Figure 2. Long total echo times led to a reduction in signals from macromolecules and lipids and, thereby, higher signal intensities of numerous water-soluble metabolites. In the spectra of CLN1 tissues compared with spectra of control subjects and CLN3 autopsy tissues, γ-aminobutyric acid (GABA) could not be detected in any of the spectra of CLN1 tissue, whereas NAA was undetectable in seven of the nine spectra, and acetate could not be detected in six of the spectra. Glutamate could not be detected in two of the spectra and was considerably reduced in the other spectra (Fig. 2A). Intensities of the glutamine signals did, however, vary among samples within each group. The spectra of CLN3 frontal cortices showed no significant differences compared with those of controls. In certain spectra from CLN3 patients (Fig. 2B), cholines [glycerophosphocholine (GPC), phosphocholine (PC), and choline (Cho)] at

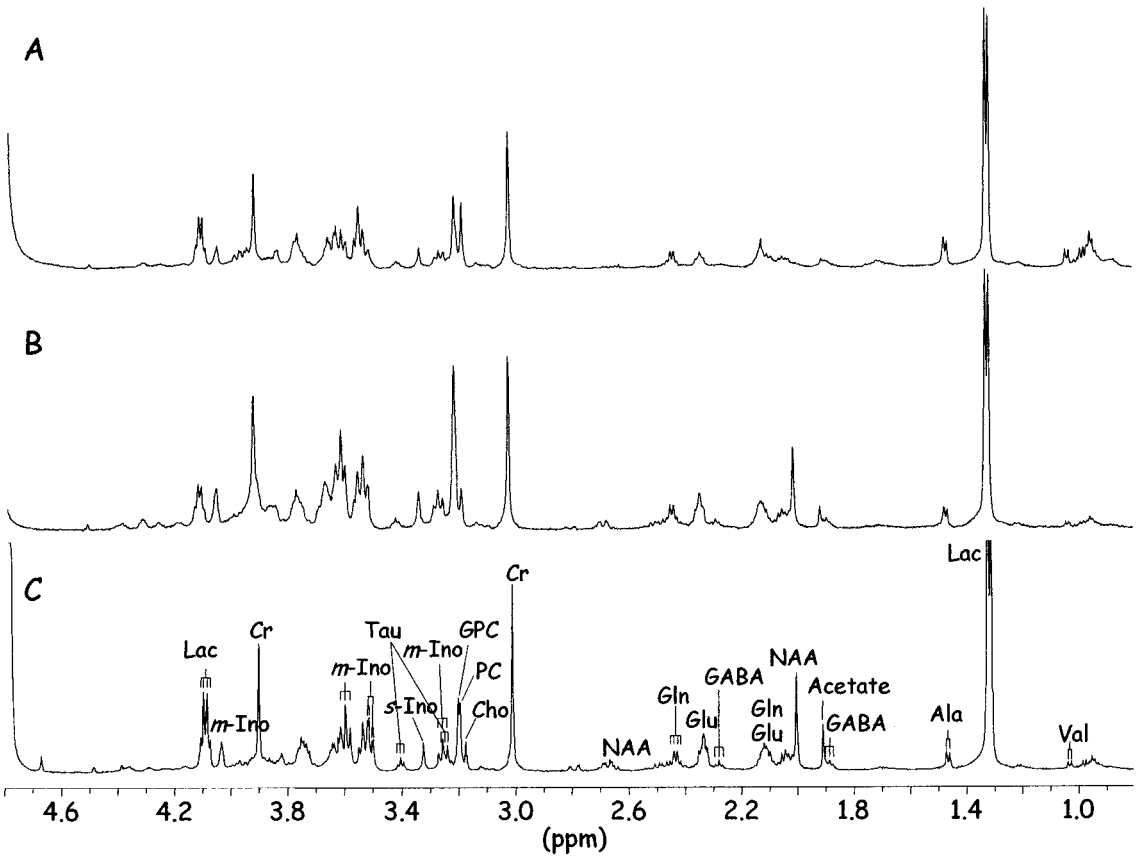

Fig. 2. HR MAS ^{1}H MR spectra at 14.7 T (600 MHz) of autopsy samples from a typical CLN1 (**A**) and CLN3 (**B**) patient and from a control subject (**C**). The CLN1 spectrum is extremely abnormal. In general, the spectra of CLN3 patients did not differ significantly from those of controls. However, in certain spectra, as shown in B, the area of GPC, PC, and Cho at 3.2 ppm appears to be elevated compared with spectra from controls. Lac, lactate; m-Ino, myo-inositol; Cr, creatine; Tau, taurine; s-Ino, scyllo-inositol; GPC, glycerophosphocholine; PC, phosphocholine; Cho, choline; NAA, *N*-acetyl-aspartate; Gln, glutamine; Glu, glutamate; GABA, γ-aminobutyrate; Ala, alanine; Val, valine.

3.2 ppm appeared to be elevated compared with controls (Fig. 2C), but these differences were not consistent.

PCA of spin echo HR MAS ^{1}H MR spectra showed that autopsy samples from patients with CLN1 had a metabolic profile different from that of the autopsy samples from controls and patients with CLN3. Statistical representation of the data was obtained by the score plot of the first (PC1) and second (PC2) principal components from PCA of spin echo HR MAS ^{1}H MR spectra, explaining 66% of the total variation in the 25 original spectra, as shown in Figure 3. In the score plot, the CLN1 samples were linearly separated from the CLN3 and control samples, whereas CLN3 and control samples were not separable. The loading profile of PC1 showed the important features characterizing most CLN1 autopsy samples (Fig. 4). The intense signals from m-Ino, scyllo-inositol (s-Ino), and GPC indicated that these compounds dominated the spectra from CLN1 patients. Furthermore, glutamine, glutamate, GABA, NAA, and acetate appeared as negative peaks in the loading profile, demonstrating the low levels of these compounds in autopsy samples from

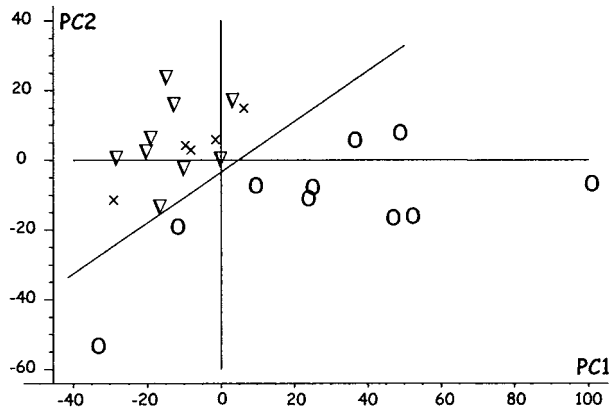

Fig. 3. Score plot from principal component analysis of spin echo HR MAS ^{1}H MR spectra with total echo time of 285 msec. Samples from controls (triangles), samples from CLN3s (crosses), and samples from CLN1s (circles) are labeled. A line is drawn to illustrate the classification of the CLN1 samples.

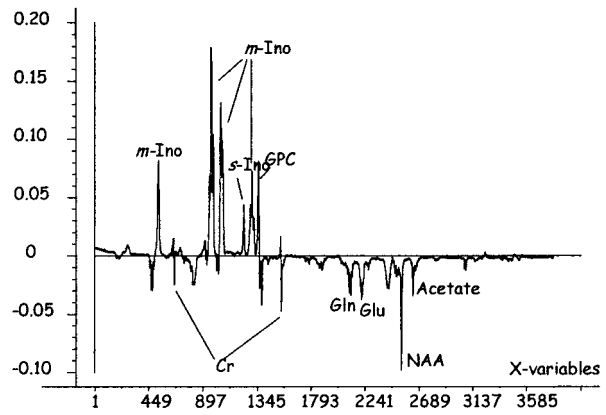

Fig. 4. Loading profile of spin echo HR MAS ^{1}H MR spectra corresponding to the spectral region of 4.6–0.6 ppm of first principal component (PC1) presented in Figure 3. The abbreviations of assignments correspond to the abbreviations used in Figure 2. The lactate peak at 1.3 ppm is excluded.

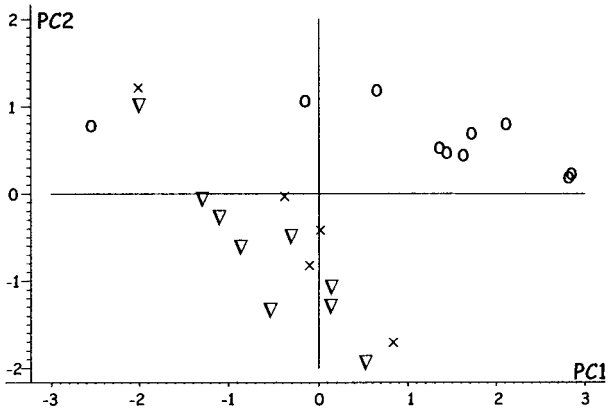

Fig. 5. Score plot of PC1 and PC2 from principal component analysis of the spectral region 3.5–0.8 ppm from single pulse water-suppressed spectra. Samples from controls (triangles), samples from CLN3s (crosses), and samples from CLN1s (circles) are labeled.

CLN1 patients compared with autopsy samples from controls and CLN3 patients.

PCA of the single pulse water-suppressed spectra also led to differentiation of the CLN1 samples from the other samples. The score plot of PC1 vs. PC2, resulting from PCA of single pulse water-suppressed spectra, is given in Figure 5. PC1 and PC2 account for 63% of the total variation in these spectra where lipids and macromolecules were detected in addition to the smaller molecules. The grouping of samples from CLN1 patients in the upper right quadrant of the score plot was evident. Furthermore, the control samples tended to score lower in PC1 and PC2 than CLN3 samples, but, as in PCA of spin echo spectra, CLN3 samples and control samples were not separable. The loading profile of PC1 (Fig. 6) showed that CLN1 samples, which had a high score for PC1, were characterized by increased relative levels of Cr, m-Ino, s-Ino, and cholines as well as decreased levels of NAA and acetate compared with controls and CLN3 samples. In addition, the loading profile of PC1 showed that the ratio of methylene/methyl protons of lipids was lower in CLN1 samples than in the other samples.

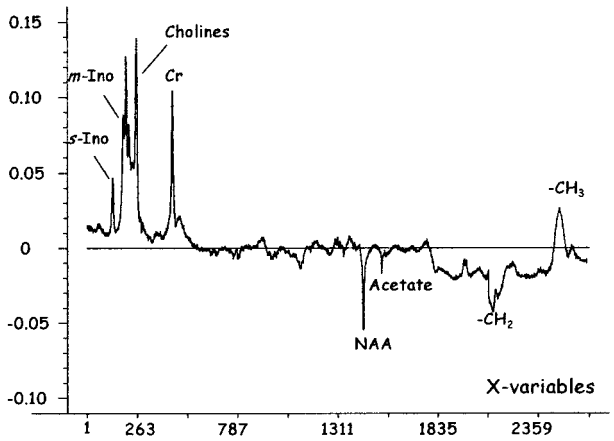

Fig. 6. Loading profile of first principal component (PC1), corresponding to the spectral region 3.5–0.8 ppm from single pulse water-suppressed spectra. The lactate peak at 1.32 ppm was excluded from the analysis. The abbreviations of assignments correspond to the abbreviations used in Figure 2, and lipid methyl- and methylene-groups are labeled $-CH_3$ and $-CH_2$ respectively.

Single pulse water-suppressed HR MAS ^{1}H MR spectra were used to analyze the lipid signals further in the CLN1, CLN3, and control brain tissue (the region of 1.8–0.5 ppm). The ratio of methylene/methyl protons of lipids was found to be significantly ($P < .01$) decreased in CLN1 tissue (CH_2/CH_3 ratio 1.32) compared with CLN3 (CH_2/CH_3 ratio 2.33) and control (CH_2/CH_3 ratio 2.52) tissues.

DISCUSSION

In Vivo ^{1}H MRS

Our in vivo ^{1}H MRS study showed a dramatic loss of NAA, a reduction of Cr, and a proportional elevation of m-Ino and lipids in the patients with CLN1. These observations are in good accordance with a previous study on one patient with CLN1, except that we did not observe an increase in taurine (Confort-Gouny et al., 1993). NAA is used as a neuronal marker, Cr is involved in energy metabolism, and Cho reflects membrane phospholipid turnover, whereas m-Ino is a glial marker and a potential osmoregulator (Yuan et al., 1992; Brand et al., 1993; Monge et al., 1993; Kuhmonen et al., 1994; Baslow, 2002). Thus, the present findings reflect the almost complete neuronal loss and extreme gliosis typical of CLN1 (Santavuori et al., 2000). The spectra of the 13 patients with CLN3 were very similar to those of controls. This observation is in accordance with the findings of Brockman et al. (1996), who examined three patients with CLN3 by using in vivo MRS.

Ex Vivo ^{1}H HR MAS MRS

In good agreement with the in vivo data, PCA of the HR MAS ^{1}H MR spectra showed altered concentrations of NAA, Cr, cholines, m-Ino, and s-Ino in the CLN1 samples. In addition, ex vivo HR MAS ^{1}H MRS allowed refined detection of two neurotransmitters, glutamate and GABA. The observed decrease in the levels of GABA and glutamate in CLN1 correspond well to the decrease in NAA, reflecting the extreme neuronal loss. Previously, markedly low cerebrospinal fluid GABA concentrations in patients with CLN1 have been reported (Riikonen et al., 2000). It seems that the concentration of GABA is decreased more significantly than that of glutamate. Imbalance between the inhibition (GABA) and the excitation (glutamate) could explain the severe myoclonic epilepsy, which is a common symptom in CLN1. Furthermore, the patients with CLN1 respond well clinically to GABAergic drugs such as sodium valproate, bentzodiazipines, and baclophen.

Furthermore, the loading profile of PC1 from PCA and peak area calculations (peak fitting) of single pulse spectra (water suppressed) showed that the ratio of methylene/methyl protons of lipids was lower in CLN1 samples than in the control or CLN3 samples. These results may indicate shorter chain lengths or a higher content of double bonds in the fatty acids. The recent results obtained using liquid chromatography-electrospray ionization mass spectrometry have shown that, indeed, the proportion of saturated short-chain fatty acids in phospholipids was increased in CLN1 autopsy brains but not in CLN3 brains (Käkelä et al., 2003), in agreement with the present results. In the PCA score plots, the CLN3 autopsy samples tend to appear closer to CLN1 samples than controls (Figs. 3, 5). However, in agreement with the in vivo data, the HR MAS ^{1}H MR spectra of CLN3 autopsy samples did not show significant differences compared with controls. This is somewhat surprising; the terminal stage of CLN3 is characterized by moderate neuronal loss and gliosis, also observed via MRI (Autti et al., 1996). The relatively normal value of NAA in the CLN3 patients might partially be explained by pseudonormalization of the NAA concentration, as discussed below.

Methodological Considerations

Autopsy material from normal children or young adults is rarely available. Therefore, the mean age of the ex vivo control group was considerably higher than that of either patient group. However, insofar as NCL diseases are considered as models of ageing (Armstrong and Koppang, 1981), the old controls were relevant in this study.

In the present study, the ex vivo HR MAS ^{1}H MR spectra were recorded from the gray matter of the frontal cortex, whereas the in vivo spectra were recorded from the deep gray matter of thalami. The CLN1 brains are extremely atrophic, the brain weight being only 300–350 g at the time of death (Haltia et al., 1973). In these shrunken brains, the thalami are best preserved, and the cerebral cortex is extremely thin (Fig. 1D). Therefore, the in vivo spectra were recorded from the thalamus, which was unfortunately not available for the ex vivo analysis. Minor metabolite differences between the deep gray matter and cortical gray matter cannot be excluded. Despite this, the ex vivo findings were in good agreement with the in vivo findings.

The HR MAS ^{1}H MRS of the brain autopsy samples was performed at room temperature, and tissue samples were subject to room temperature for 25 min on average before MR spectra were recorded. Under these conditions, anaerobic respiration and degradation of tissue metabolites is likely to occur. Indeed, the signal intensities of lactate, which reflects the anaerobic respiration (Wolfson et al., 2000), were high in HR MAS ^{1}H MR spectra compared with in vivo spectra, and therefore lactate was not included in the data analysis. Also, acetate was observable. Cheng et al. (1997) showed evidence indicating that, in autopsy brains, acetate is mostly produced by degradation of NAA. There was an inverse correlation between the post-mortem delay time and NAA concentration, so Cheng et al. suggested that the initial NAA concentration in the tissue can best be estimated by summarizing the NAA and acetate signals. In the CLN1 tissues, both NAA and acetate were decreased, although they were similar to controls in CLN3 tissues.

NAA in Neurodegeneration

The decreased level of NAA has been associated with neuronal damage or loss (Burtscher and Holtås, 2001; Vermathen et al., 2003; Baslow, 2003), and an inverse correlation of the tissue NAA concentration and neuronal loss has been demonstrated in Pick's and Alzheimer's diseases (Cheng et al., 1997, 2002). In the CNS, NAA is synthesized and stored in neurons but is catabolized in oligodendrocytes. Increasing recent evidence indicates that one important role of the NAA intercompartmental cycle is osmoregulatory, by removing intracellular water from myelinated neurons (Baslow and Guilfoyle, 2002; Baslow, 2003; Baslow et al., 2003). In CLN1, the neuronal loss is extreme, so the dramatic decrease of neuronal metabolites, including NAA, was expected. However, it is somewhat surprising that, despite the well-documented moderate cerebrocortical neurodegeneration (Haltia, 2003), the samples from patients with CLN3 failed to show significant alterations in the concentration of NAA. This might be partially explained by the fact that, in the CLN3 brains, the remaining neurons are filled with storage material (Haltia, 2003), and osmotic imbalance may exist, potentially leading to compensation of the NAA concentration via up-regulation. If this is the case, then the NAA concentration might not directly reflect the degree of neurodegeneration in lysosomal storage diseases with potential osmotic imbalance. Indeed, we are aware of one further example fitting this theory: In vivo MRS studies of patients with aspartylglucosaminuria, showing mild to moderate cortical atrophy, indicated NAA concentrations within the normal range (Autti and Häkkinen, unpublished results).

CONCLUSIONS

In the present study, we show that the results obtained from in vivo ^{1}H MR spectra and ex vivo HR MAS ^{1}H MR spectra of patients with CLN1 and CLN3 and controls were in good agreement. The PC1 loading profile of CLN1 samples was characterized by the intense positive peaks from m-Ino, s-Ino, and GPC and by the negative peaks of glutamine, glutamate, GABA, NAA, and acetate. Also, the ratio of lipid methylene/methyl protons was lower in CLN1 samples than in the other samples. Thus, despite the necessary post-mortem delay, ^{1}H HR MAS MRS provided a reliable technical ability to analyze the metabolic profiles in autopsy brain tissue and allowed refined detection of metabolites such as GABA and glutamate as well as knowledge of lipid composition in CLN1 and CLN3 brains. HR MAS ^{1}H MR spectra allowed clear differentiation of the CLN1 samples from the CLN3 and control samples, whereas the CLN3 and control samples were not separable.

ACKNOWLEDGMENTS

The authors thank Dr. Riitta Salonen for support in this study. We would like to dedicate this paper to the memory of our dear friend and coworker, Professor Pirk ko Santavuori, who passed away on February 6, 2004.

REFERENCES

Armstrong D, Koppang N. 1981. Ceroid-lipofucinosis, a model for aging. In: Sohal RS, editor. Age pigments. Amsterdam: Elsevier, p 355–382.

Autti T, Raininko R, Vanhanen SL, Santavuori P. 1996. MRI of neuronal ceroid lipofuscinosis. I. Cranial MRI of 30 patients with juvenile neuronal ceroid lipofuscinosis. Neuroradiology 38:476–482.

Autti T, Raininko R, Vanhanen SL, Santavuori P. 1997. Magnetic resonance techniques in neuronal ceroid lipofuscinoses and some other lysosomal diseases affecting the brain. Curr Opin Neurol 10:519–524.

Barton SJ, Howe FA, Tomlins AM, Cudlip SA, Nicholson JK, Bell BA, Griffiths JR. 1999. Comparison of in vivo ^{1}H MRS of human brain tumours with ^{1}H HR-MAS spectroscopy of intact biopsy samples in vitro. Magma 8:121–128.

Baslow MH. 2003. N-acetylaspartate in the vertebrate brain: metabolism and function. Neurochem Res 28:941–953.

Baslow MH, Guilfoyle DN. 2002. Effect of *N*-acetylaspartic acid on the diffusion coefficient of water: a proton magnetic resonance phantom method for measurement of osmolyte-obligated water. Anal Biochem 311:133–138.

Baslow MH, Suckow RF, Gaynor K, Bhakoo KK, Marks N, Saito M, Saito M, Duff K, Matsuoka Y, Berg MJ. 2003. Brain damage results in down-regulation of *N*-acetylaspartate as a neuronal osmolyte. Neuromol Med 3:95–104.

Brand A, Richter-Landsberg C, Leibfritz D. 1993. Multinuclear NMR studies on the energy metabolism of glial and neuronal cells. Dev Neurosci 15:289–298.

Brockmann K, Pouwels PJ, Christen HJ, Frahm J, Hanefeld F. 1996. Localized proton magnetic resonance spectroscopy of cerebral metabolic disturbances in children with neuronal ceroid lipofuscinosis. Neuropediatrics 27:242–248.

Burtscher IM, Holtås S. 2001. Proton MR spectroscopy in clinical routine. J Magn Reson Imag 13:560–567.

Cheng LL, Ma MJ, Becerra L, Ptak T, Tracey I, Lackner A, González RG. 1997. Quantitative neuropathology by high resolution magic angle spinning proton nuclear magnetic resonance spectroscopy. Proc Natl Acad Sci USA 94:6408–6413.

Cheng LL, Chang IW, Smith BL, Gonzalez RG. 1998. Evaluating human breast ductal carcinomas with high-resolution magic-angle spinning proton magnetic resonance spectroscopy. J Magn Res 135:194–202.

Cheng LL, Anthony DC, Comite AR, Black PM, Tzika AA, González RG. 2000. Quantification of microheterogeneity in glioblastoma multiforme with ex vivo high-resolution magic-angle spinning (HRMAS) proton magnetic resonance spectroscopy. Neurooncology 2:87–95.

Cheng LL, Wu C, Smith MR, Gonzalez RG. 2001. Non-destructive quantitation of spermine in human prostate tissue samples using HRMAS ^{1}H NMR spectroscopy at 9.4 T. FEBS Lett. 494:112–116.

Cheng LL, Newell K, Mallory AE, Hyman BT, Gonzalez RG. 2002. Quantification of neurons in Alzheimer and control brains with ex vivo high resolution magic angle spinning proton magnetic resonance spectroscopy and stereology. Magn Reson Imag 20:527–533.

Confort-Gouny S, Chabrol B, Vion-Dury J, Mancini J, Cozzone PJ. 1993. MRI and localized proton MRS in early infantile form of neuronal ceroid- lipofuscinosis. Pediatr Neurol 9:57–60.

Gao H, Boustany RM, Espinola JA, Cotman SL, Srinidhi L, Antonellis KA, Gillis T, Qin X, Liu S, Donahue LR, Bronson RT, Faust JR, Stout D, Haines JL, Lerner TJ, MacDonald ME. 2002. Mutations in a novel CLN6-encoded transmembrane protein cause variant neuronal ceroid lipofuscinosis in man and mouse. Am J Hum Genet 70:324–335.

Gonzalez RG, Cheng LL, Westmoreland SV, Sakaie KE, Becerra LR, Lee PL, Masliah E, Lackner AA. 2000. Early brain injury in the SIV-macaque model of AIDS. AIDS 14:2841–2849.

Haltia M. 2003. The neuronal ceroid-lipofuscinoses. J Neuropathol Exp Neurol 62:1–13.

Haltia M, Rapola J, Santavuori P. 1973. Infantile type of so-called neuronal ceroid-lipofuscinosis. Histological and electron microscopic studies. Acta Neuropathol 26:157–170.

Hofmann SL, Peltonen L. 2001. The neuronal ceroid lipofuscinoses. In: Scriver CR, Beaudet AL, Sly WS, Valle D, editors. The metabolic and molecular bases of inherited disease, vol III, 8th ed. Columbus, OH: McGraw-Hill Companies Inc. p 3877–3894.

International Batten Disease Consortium. 1995. Isolation of a novel gene underlying Batten disease, CLN3. Cell 82:949–957.

Järvelä I, Autti T, Lamminranta S, Aberg L, Raininko R, Santavuori P. 1997. Clinical and magnetic resonance imaging findings in Batten disease: analysis of the major mutation (1.02-kb deletion). Ann Neurol 42:799–802.

Järvi J, Nyman S, Komu M, Forsström JJ. 1997. A PC program for automatic analysis of NMR spectrum series. Comput Methods Programs Biomed 52:213–222.

Käkelä R, Somerharju P, Tyynelä J. 2003. Analysis of phospholipid molecular species in brains from patients with infantile and juvenile lipofuscinosis using liquid chromatography-electrospray ionization mass spectrometry. J Neurochem 84:1051–1065.

Kuhmonen J, Sivenius J, Riekkinen PJ Sr, Kauppinen RA. 1994. Decrease in brain choline-containing compounds following a short period of global ischemia in gerbils as detected by ^{1}H NMR spectroscopy in vivo. NMR Biomed 7:231–236.

Lauronen L, Munroe PB, Järvelä I, Autti T, Mitchison HM, O'Rawe AM, Gardiner RM, Mole SE, Puranen J, Häkkinen AM, Kirveskari E, Santavuori P. 1999. Delayed classic and protracted phenotypes of compound heterozygous juvenile neuronal ceroid lipofuscinosis. Neurology 52:360–365.

Mole SE. 1999. Batten's disease: eight genes and still counting? Lancet 354:443–445.

Monge M, Yuan J, Cabon F, Zalc B, Kanfer JN. 1993. Glycerophosphorylcholine phosphocholine phosphodiesterase activity during the differentiation of glial progenitor cells. J Neurosci Res 36:441–445.

Polvikoski T, Sulkava R, Myllykangas L, Notkola IL, Niinisto L, Verkkoniemi A, Kainulainen K, Kontula K, Perez-Tur J, Hardy J, Haltia M. 2001. Prevalence of Alzheimer's disease in very elderly people: a prospective neuropathological study. Neurology 56:1690–1696.

Ranta S, Zhang Y, Ross B, Lonka L, Takkunen E, Messer A, Sharp J, Wheeler R, Kusumi K, Mole S, Liu W, Soares MB, Bonaldo MF, Hirvasniemi A, de la CA, Gilliam TC, Lehesjoki AE. 1999. The neuronal ceroid lipofuscinoses in human EPMR and mnd mutant mice are associated with mutations in CLN8. Nat Genet 23:233–236.

Riikonen R, Vanhanen SL, Tyynela J, Santavuori P, Turpeinen U. 2000. CSF insulin-like growth factor-1 in infantile neuronal ceroid lipofuscinosis. Neurology 54:1828–1832.

Santavuori P. 1988. Neuronal ceroid lipofuscinoses in childhood. Brain Dev 10:80–83.

Santavuori P, Lauronen L, Kirveskari E, Åberg L, Sainio K, Autti T. 2000. Neuronal ceroid lipofuscinoses in childhood. Neurol Sci 21:S35–S41.

Savukoski M, Klockars T, Holmberg V, Santavuori P, Lander ES, Peltonen L. 1998. CLN5, a novel gene encoding a putative transmembrane protein mutated in Finnish variant late infantile neuronal ceroid lipofuscinosis. Nat Genet 19:286–288.

Seitz D, Grodd W, Schwab A, Seeger U, Klose U, Nägele T. 1998. MR imaging and localized proton MR spectroscopy in late infantile neuronal ceroid lipofuscinosis. Am J Neuroradiol 19:1373–1377.

Sitter B, Sonnewald U, Spraul M, Fjosne HE, Gribbestad IS. 2002. High-resolution magic angle spinning MRS of breast cancer tissue. NMR Biomed 15:327–337.

Sleat DE, Donnelly RJ, Lackland H, Liu CG, Sohar I, Pullarkat RK, Lobel P. 1997. Association of mutations in a lysosomal protein with classical late- infantile neuronal ceroid lipofuscinosis. Science 277:1802–1805.

Taylor JL, Wu CL, Cory D, Gonzalez RG, Bielecki A, Cheng LL. 2003. High-resolution magic angle spinning proton NMR analysis of human prostate tissue with slow spinning rates. Magn Reson Med 20:627–632.

Tzika AA, Cheng LL, Goumnerova L, Madsen JR, Zurakowski D, Astrakas LG, Zarifi MK, Scott RM, Anthony DC, Gonzalez RG, Black PM. 2002. Biochemical characterization of pediatric brain tumors by using in vivo and ex vivo magnetic resonance spectroscopy. J Neurosurg 96:1023–1031.

Vermathen P, Laxer KD, Schuff N, Matson GB, Weiner MW. 2003. Evidence of neuronal injury outside the medial temporal lobe in temporal lobe epilepsy: *N*-acetylaspartate concentration reductions detected with multisection proton MR spectroscopic imaging—initial experience. Radiology 226:195–202.

Vesa J, Hellsten E, Verkruyse LA, Camp LA, Rapola J, Santavuori P, Hofmann SL, Peltonen L. 1995. Mutations in the palmitoyl protein thioesterase gene causing infantile neuronal ceroid lipofuscinosis. Nature 376:584–587.

Wheeler RB, Sharp JD, Schultz RA, Joslin JM, Williams RE, Mole SE. 2002. The gene mutated in variant late-infantile neuronal ceroid lipofuscinosis (CLN6) and in nclf mutant mice encodes a novel predicted transmembrane protein. Am J Hum Genet 70:537–542.

Wolfson M, Bersudsky Y, Hertz E, Berkin V, Zinger E, Hertz L. 2000. A model of inositol compartmentation in astrocytes based upon efflux kinetics and slow inositol depletion after uptake inhibition. Neurochem Res 25:977–982.

Yuan J, McCartney DG, Monge M, Espinosa de Los MA, Zalc B, de Vellis J, Kanfer JN. 1992. Glycerophosphorylcholine phosphocholine phosphodiesterase activity in cultured oligodendrocytes, astrocytes, and central nervous tissue of dysmyelinating rodent mutants. J Neurosci Res 31:68–74.